Proceedings of the 7th International Symposium on Steel Science (ISSS 2024)
Nov. 11-14, 2024, Kyoto, Japan: The Iron and Steel Institute of Japan

Improvement of fatigue limit by pre-fatigue deformation in 1.6 GPa-grade as-quenched martensitic steel

Kazuho Okada[1*], Eri Nakagawa[1], Kaneaki Tsuzaki[1], Akinobu Shibata[1]

[1] Research Center for Structural Materials, National Institute for Materials Science (NIMS), 1-2-1 Sengen, Tsukuba 305-0047, Japan.

Abstract: The fatigue limit of steel generally increases with tensile strength; however, when tensile strength exceeds ~1.4 GPa, further increases in tensile strength fail to elevate the fatigue limit or may even decrease it (fatigue limit ceiling). This ceiling poses a challenge for the widespread application of ultrahigh-strength steels. In this study, we successfully achieved a significant improvement in the fatigue limit through pre-fatigue deformation, thereby breaking through the fatigue limit ceiling in 1.6 GPa-grade as-quenched martensitic steel (Fe-3Mn-0.2C (wt.%)). The maximum stress corresponding to the fatigue limit increased from 675 MPa to 1300 MPa (stress ratio: 0.1, 10^7 cycles). In contrast, a specimen subjected to pre-constant-loading at the same maximum stress as the pre-fatigue training showed only minimal improvement in the fatigue limit. These findings reveal that fatigue deformation, traditionally viewed as detrimental, can be beneficial for fatigue fracture resistance when properly applied. Moreover, the absence of surface cracks in all non-fractured specimens indicates that the fatigue limit of as-quenched martensitic steels aligns with the crack initiation limit, rather than the crack non-propagation limit. Therefore, the significant improvement in the fatigue limit is attributed to the improvement in the crack initiation limit achieved through the pre-fatigue deformation.

1. BACKGROUND

Fatigue failure, which accounts for approximately 80% of structural failure accidents, poses a significant obstacle to achieving further high strength in steels [1]. Generally, the fatigue limit (σ_W, expressed by stress amplitude) of steel increases with the tensile strength (σ_B). However, it has been reported that beyond a σ_B of approximately 1.4 GPa, further increases in σ_B fail to elevate the σ_W or may even decrease it (so-called fatigue limit ceiling). Consequently, the practical application of ultrahigh-strength steels with a σ_B exceeding 1.5 GPa is highly restricted, necessitating the development of material design guidelines to break through the fatigue limit ceiling. The σ_W corresponds to the greater of the "crack initiation limit" and the "crack non-propagation limit", and, for the majority of steels, the σ_W corresponds to the crack non-propagation limit [2]. Thus, the fatigue limit ceiling can be considered as the ceiling of the crack non-propagation limit. In this study, we challenged to break through the fatigue limit ceiling by improving the crack initiation limit, rather than the crack non-propagation limit.

Lath martensite structure is a characteristic microstructure in high-strength low/medium-carbon steels. It is well known that lath martensite satisfies the Kurdjumov-Sachs (K-S) orientation relationship relative to the parent austenite, related to the subdivision of a prior austenite grain into several structural units with different size scales, namely lath, block, and packet. Block boundaries, packet boundaries, and prior austenite grain boundaries (PAGB) are basically high-angle boundaries, while lath boundaries are low-angle boundaries [3, 4]. The σ_W of tempered martensitic steels is generally around 42% of σ_B, while that of as-quenched martensitic steel typically achieves approximately 27% or lower for a stress ratio (R) of 0 at σ_B < ~1.4 GPa [5–9]. Therefore, tempered martensitic steels, whose σ_B is reduced from as-quenched conditions, are practically applied for structural components. However, the reason for the low σ_W of as-quenched martensitic steel remains unclear. If martensitic steels could be widely applied in its highest-strength as-quenched conditions, it would be expected to contribute to a sustainable society by improving the fuel efficiency of transportation equipment such as automobiles. This study attempted to break through the fatigue limit ceiling in as-quenched martensitic steel by improving the crack initiation limit using pre-fatigue deformation.

* Corresponding author. E-mail: okada.kazuho@nims.go.jp, telephone: +81 29 859 2630.

https://doi.org/10.2355/isijisss.2024.0_201

2. EXPERIMENTAL PROCEDURE

In this study, we used an Fe-3Mn-0.2C ingot with the following composition: Mn 3.02, C 0.18, Si 0.01, P <0.002, S 0.001, Al 0.002, N 0.002, O 0.001, and Fe: balance (wt.%). The hot-rolled plate, originally 18 mm thick, was cold-rolled to a thickness of 1.8 mm, achieving a 90% thickness reduction. The cold-rolled sheet was then austenitized at 900 ℃ for 30 min, followed by ice brine quenching and sub-zero cooling in liquid nitrogen for 10 min.

Sheet-type smooth specimens with gauge dimensions of 1 mm in thickness, 4 mm in width, and 8 mm in gauge length were prepared from the as-heat-treated specimen. These sheet-type specimens were mechanically polished using emery paper up to #4000 grid, and then electrochemically polished in an aqueous solution of 50 ml $HCLO_4$ + 450 ml CH_3COOH for 90 s (referred to as "non-deformed specimen"). The non-deformed specimen was then subjected to uniaxial fatigue deformation with a frequency of 50 Hz, maximum stress (s_{max}) of 1000 MPa, and stress amplitude of 50 MPa (R = 0.9, referred to as "pre-fatigued specimen") for 10^7 cycles. The other non-deformed specimen was subjected to constant load with 1000MPa (referred to as "pre-constant-loaded specimen") for 2×10^5 s which is the same time of 10^7 cycles with 50Hz. The surface layer, 20 to 30 μm thickness, was removed through mechanical and electrochemical repolishing (the same as the first polishing), after which a fatigue test was performed at a frequency of 50 Hz and R of 0.1 (up to 10^7 cycles). Given the submicron size of laths (single crystals) in lath martensitic structure, repolishing the 20 to 30 μm surface layer fabricates new smaller specimens from the larger specimen after pre-deformation, distinguishing this process from mere crack initiation retardation by removing intrusion/extrusion. We opted for repolishing rather than recutting fatigue specimens from larger pre-fatigued samples due to the load capacity limits of our testing machine. For the pre-fatigued specimens tested at the fatigue limit, the repolishing and fatigue testing process was repeated every 10^7 cycles, with an increase in s_{max} by 25 ~ 100 MPa, until they were fractured. We refer to the pre-fatigued specimen tested up to s_{max} of 1250 MPa as the initial microstructure of the "pre-fatigued + coaxing specimen". Additionally, we performed uniaxial tensile tests at an initial strain rate of 10^{-4} s^{-1} to evaluate elastic limit (σ_E), 0.2% proof stress (σ_Y), and σ_B. The nominal stress, at the point where the deviation between the nominal stress–nominal strain curve and the straight line extrapolated from the average slope between 50 and 250 MPa exceeds 5 MPa, was defined as the elastic limit.

3. RESULTS AND DISCUSSION

Fig.1 presents an optical microscopy image of the as-heat-treated sample, showing a lath martensitic structure with an average PAG size of 62 μm. The PAG size was measured by the line-interception method.

The tensile and fatigue properties are summarized in Table 1. The σ_B of the non-deformed, pre-constant-loaded, and pre-fatigued specimens were almost the same (~1.6 GPa), while that of the pre-fatigued + coaxing specimen was softened by approximately 100 MPa, but it was still larger than 1.5 GPa. The s_{max} corresponding to fatigue limit ($s_{max\text{-}W}$) was 675, 725, 1025, and 1300 MPa in the non-

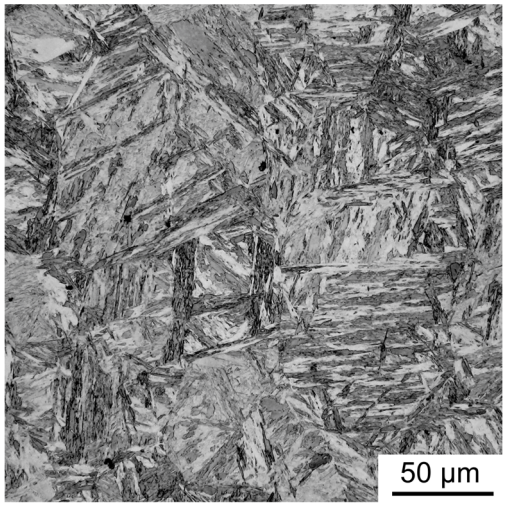

Figure 1 Optical microscopy image of the as-heat-treated sample.

Table 1 Summary of the tensile and fatigue properties

	σ_B [MPa]	σ_Y [MPa]	σ_E [MPa]	$s_{max\text{-}W}$ at R = 0.1 [MPa]	Fatigue limit for R = 0 ($\sigma_{W(0)}$) [MPa]	$\sigma_{W(0)}$ / σ_B
Non-deformed	1615	1118	378	675	317	0.20
Pre-constant loaded	1613	1324	868	725	341	0.22
Pre-fatigued	1619	1324	1070	1025	493	0.31
Prefatigued + coaxing	1501	1278	699	1300	641	0.43

deformed, pre-constant-loaded, pre-fatigued, and pre-fatigued + coaxing specimens, respectively. We converted the σ_W at R = 0.1 ($\sigma_{W(0.1)}$) to that at R = 0 ($\sigma_{W(0)}$) using the following equation (modified Goodman diagram [10]), summarized in Table 1,

$$\sigma_{W(x)} = \sigma_{W(-1)}\left(1-\frac{\sigma_{m(x)}}{\sigma_B}\right) \quad (1)$$

where $\sigma_{W(x)}$ and $\sigma_{m(x)}$ are the stress amplitude and average stress, respectively, at the fatigue limit for R = x. The $\sigma_{W(0)}/\sigma_B$ of the pre-constant-loaded specimen was 0.22, which showed only a slight improvement over that in the non-deformed specimen (0.20). On the other hand, the $\sigma_{W(0)}/\sigma_B$ was 0.31 and 0.43 in the pre-fatigued and pre-fatigued + coaxing specimens, respectively. Notably, the $\sigma_{W(0)}/\sigma_B$ of the pre-fatigued + coaxing specimen was doubled compared to the non-deformed specimen, surpassing the fatigue limit ceiling. The results demonstrate that fatigue deformation, traditionally viewed as detrimental, can be beneficial for fatigue fracture resistance when properly applied. In addition, we carefully observed the specimens' surfaces after the fatigue test at the $s_{max\text{-}W}$. However, no surface crack was observed in all the non-fractured specimens, suggesting that the fatigue limit of the as-quenched martensitic steels corresponded to the crack initiation limit, not the crack non-propagation limit. Therefore, we concluded that the pre-fatigue training improved the crack initiation limit and led to the significant improvement in the fatigue limit. This phenomenon is completely different from the conventional coaxing effect, where, particularly in carbon steels, the dynamic strain aging of carbon hardens the non-propagation crack tip area and improves the ability to terminate crack propagation [11, 12].

Fig.2 shows the relationship between the $s_{max\text{-}W}$ and the (a) σ_Y or (b) σ_E. The significant improvement in the $s_{max\text{-}W}$ is not consistent with the values of σ_Y and σ_E, supporting the fatigue limit corresponding to the crack initiation limit. The crack non-propagation limit is basically proportional to the bulk average properties, such as σ_B, σ_Y, and σ_E, because crack termination can occur anywhere within a material [13]. In contrast, crack initiation can occur at the weakest domain in a material, which cannot be evaluated from the bulk average properties. Therefore, understanding the fatigue crack initiation mechanism, i.e., identifying the weakest domain, is expected to clarify the origin of the significant improvement in the fatigue limit by pre-fatigue deformations.

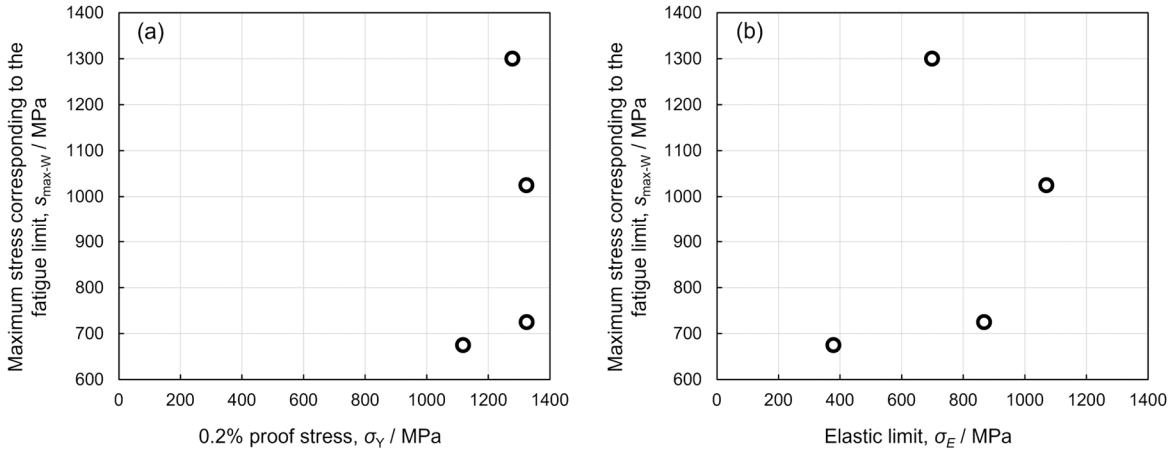

Figure 2 Relationship between the $s_{max\text{-}W}$ and the (a) σ_Y or (b) σ_E.

4. CONCLUSION

This study attempted to break through the fatigue limit ceiling in as-quenched martensitic steel by improving the crack initiation limit using pre-fatigue deformation. The major conclusions are as follows.

1. We successfully doubled the fatigue limit of 1.6 GPa-grade as-quenched martensitic steel, suggesting that fatigue deformation, traditionally viewed as detrimental, can strengthen materials when properly applied.
2. The fatigue limit of the as-quenched martensitic steels corresponded to the crack initiation limit, not the crack non-propagation limit. Therefore, the pre-fatigue training improved the crack initiation limit and led to the significant improvement in the fatigue limit.
3. The significant improvement in fatigue limit does not originate from the change in the bulk average properties, such as tensile strength, proof stress, and elastic limit.

Acknowledgments: This study was financially supported by the Japan Science and Technology Agency ACT-X grant (JPMJAX23D5) and the Japan Society for the Promotion of Science KAKENHI grant (JP23K13541, JP23H01717 and JP23K26410).

REFERENCES

[1] H. Mughrabi: Philosophical Transactions of the Royal Society A, 373 (2015), e20140132.
[2] N.E. Frost, K.J. Marsh, L.P. Pook: Metal Fatigue, Oxford University (1974).
[3] S. Morito, X. Huang, T. Furuhara, T. Maki, N. Hansen: Acta Materialia, 54 (2006), 5323–5331.
[4] A. Shibata, G. Miyamoto, S. Morito, A. Nakamura, T. Moronaga, H. Kitano, I. Gutierrez-Urrutia, T. Hara, K. Tsuzaki: Acta Materialia, 246 (2023), e118675.
[5] NIMS Fatigue Data Sheet No.115: https://fds.nims.go.jp/
[6] N. Iwata, Y. Tomota, K. Katahira, H. Suzuki: Materials Science and Technology, 18 (2022), 629–632.
[7] K. Okada, A. Shibata, Y. Takeda, N. Tsuji: International Journal of Fatigue, 143 (2021), e105921.
[8] H. Matsumiya, A. Shibata, K. Okada, N. Tsuji: International Journal of Hydrogen Energy, 46 (2021), 37509–37517.
[9] K. Monma, H. Sudo: Journal of the Japan Institute of Metals and Materials, 27 (1963), 125–130.
[10] T. Nicholas, J. R. Zuiker: International Journal of Fracture, 80 (1996), 219–235.
[11] T. Yakushiji, M. Kage and H. Nisitani: Transactions of the Japan Society of Mechanical Engineers Series A, 62 (1996), 82–88.
[12] M. Koyama, B. Ren, N. Yoshimura, E. Sakurada, K. Ushioda, H. Noguchi: ISIJ International, 57 (2017), 358–364.
[13] Y. Murakami, M. Endo: International Journal of Fatigue, 16 (1994), 163–182.